RSC Advances

PAPER

View Article Online
View Journal | View Issue

Cite this: *RSC Adv.*, 2018, **8**, 35453

Mechanistic study of the ligand controlled regioselectivity in iridium catalyzed C–H borylation of aromatic imines†

Yuhua Liu,‡[a] Jipei Chen,‡[a] Kangsheng Zhan,[a] Yiqiang Shen,[a] Hui Gao *[bc] and Lingmin Yao *[a]

As a major challenge in C–H borylation, how to control the selectivity has attracted lots of attention, however, the related mechanistic information still needs to be uncovered. Herein, density functional theory (DFT) has been used to study the mechanism for the ligand controlled regioselectivity in the iridium-catalyzed C–H borylation of aromatic imines, which is inspired by experimental observations (R. Bisht, B. Chattopadhyay, *J. Am. Chem. Soc.*, 2016, **138**, 84–87). The proposed Ir(I)–Ir(III) catalytic cycle includes (i) the oxidative addition of the C–H bond to iridium(I); (ii) the reductive elimination of a C–B bond; (iii) the oxidative addition of B_2pin_2 to an iridium(I) hydride complex; and (iv) the reductive elimination of a B–H bond. The oxidative addition of a C–H bond to the iridium center is the determining step. For the ligand AQ, *ortho*-selectivity is proposed to be attributed to the decreased steric hindrance and increased electron donating effect of AQ (8-aminoquinoline) which promotes proton-transfer in the *ortho*-transition state of C–H activation. While, for the TMP ligand, the steric repulsion between the TMP (4,5,7,8-tetramethyl-1, 10-phenanthroline) ligand and the *ortho*-substituted imine hinders the *ortho* C–H activation and favors *meta* borylation. Our calculations provide insights into further ligand design to achieve different regioselective borylation of aromatics. Guided by the results, the regioselectivity in the borylation of aromatics may be achieved by accordingly modifying the electronic and steric substituents of the ligand.

Received 22nd September 2018
Accepted 10th October 2018

DOI: 10.1039/c8ra07886f

rsc.li/rsc-advances

Introduction

Transition metal catalyzed C–H borylation of aryl rings is one of the most important methods used to activate C–H bonds and functionalize organic molecules.[1] In the past years, the C–H borylation reaction catalyzed by different transition metal complexes such as Ir, Rh, and Co has been developed well.[2–6] In particular, the number of iridium catalyzed aromatic C–H borylation reactions have grown considerably,[4–7] in which an important issue to be solved is how to control the regioselectivity. One of the most employed strategies is the combination of iridium complexes with directing groups to allow selective *ortho*-borylation.[8–10] Smith reported an example of sterically directed *ortho*-borylation.[11] On the other hand, *meta*-selective C–H bond borylation of aryl rings is more difficult. Only a few methods for the sterically controlled *meta* selective borylations have been reported.[12,13]

Understanding the experimentally observed ligand controlled regioselectivity is essential for clarification of the detailed influence of ligands and guiding further catalysis design. Previous studies have proposed several hypothesises on the regioselective C–H borylation,[14–19] though debate is still existed. Maseras and co-workers suggested that in the borylation of methyl benzoate catalyzed by iridium complexes supported by PPh_3 (triphenyl phosphine) or dtbpy (4,4-di-*tert*-butyl bipyridine), the possible mechanism is iridium(III)/iridium(V) catalytic cycle[17](Fig. 1, green). Alternatively, Lan and co-workers suggested that in the borylation of aromatic C–H catalyzed by $[Ir(cod)OH]_2$/Xyl-MeO-BIPHEP, iridium(I)/iridium(III)-based catalytic cycle exists[18] (Fig. 1, aubergine).

Recently, Chattopadhyay reported a series of iridium catalyzed borylation of aromatics with diboron reagents (Scheme 1).[20] The original report described that the Ir catalysts supported by AQ showed the capability of borylation on *ortho* position of aromatic imine while the Ir/TMP system preferred *meta*-selectivity, however, no explanation on the regioselectivity was given. There are some issues to be answered: (1) what are the details of the catalytic cycle? (2) What is the regioselective determine step

[a]*School of Physics and Electronic Engineering, Guangzhou University, Guangzhou, 510006, China. E-mail: emmiyao@163.com*

[b]*Key Laboratory of Molecular Target & Clinical Pharmacology, School of Pharmaceutical Sciences & the Fifth Affiliated Hospital, Guangzhou Medical University, Guangzhou, 511436, China. E-mail: gaoh9@gzhmu.edu.cn*

[c]*Guangzhou Institute of Energy Conversion, Chinese Academy of Sciences, Guangzhou 510640, PR China*

† Electronic supplementary information (ESI) available. See DOI: 10.1039/c8ra07886f

‡ The authors contributed equally to this work.

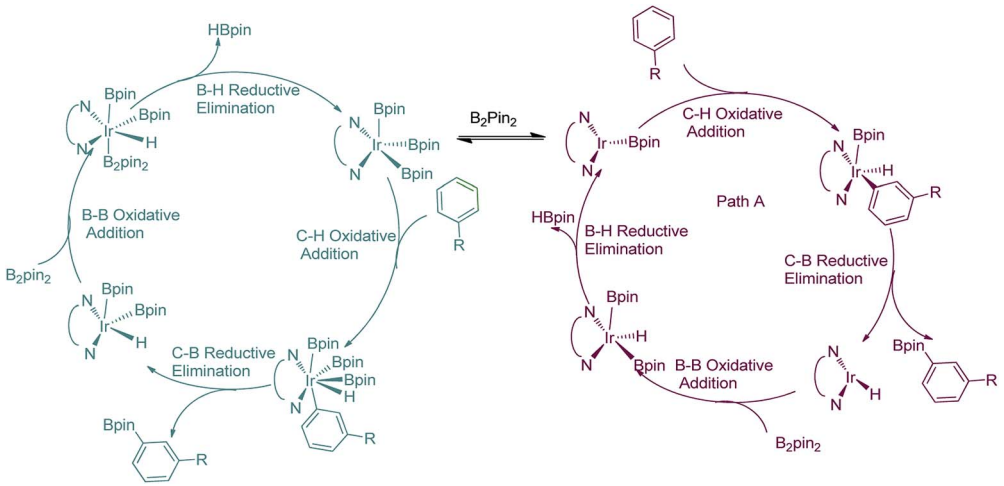

Fig. 1 Potential mechanisms of iridium(III)/iridium(V) and iridium(I)/iridium(III) catalytic cycles for aromatic C–H borylation.

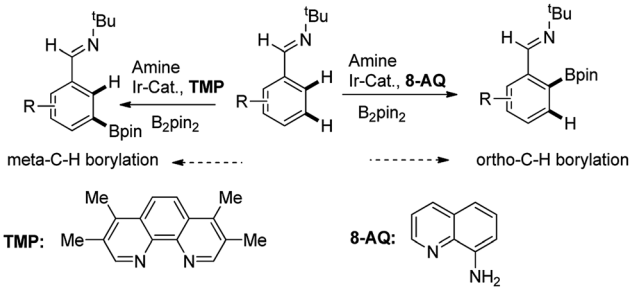

Scheme 1 Computational model for aromatic C–H borylation.

in the cycle? (3) How does the structure of ligand influence the reactivity and regioselectivity? With the aim of answering these questions, we conducted computational study by using the prototypical reaction between phenyl imine and pinacolborane as the model reaction (Scheme 1).

For the special reaction system in the model reaction (Scheme 1), three possible mechanistic pathways have been demonstrated and the related reaction profiles have been examined. All the pathways involve C–H activation, C–B reductive elimination and B–B oxidative addition and B–H reductive elimination steps. The only difference lies in that path I proceeds in the sequence of C–H activation, C–B reductive elimination, B–B oxidative addition and B–H reductive elimination (Scheme 2a); while path II occurs in the sequence of C–H activation, B–H reductive elimination, B–B oxidative addition and C–B reductive elimination (Scheme 2b). Both path I and path II proceed through Ir(I)–Ir(III) catalytic cycle. Path III undergoes the analogues reaction sequence with path I but *via* Ir(III)–Ir(V) catalytic cycle (Scheme 2c). Herein, we report our investigations on the above possible pathways with special emphasis on the ligand effects on regioselectivity.

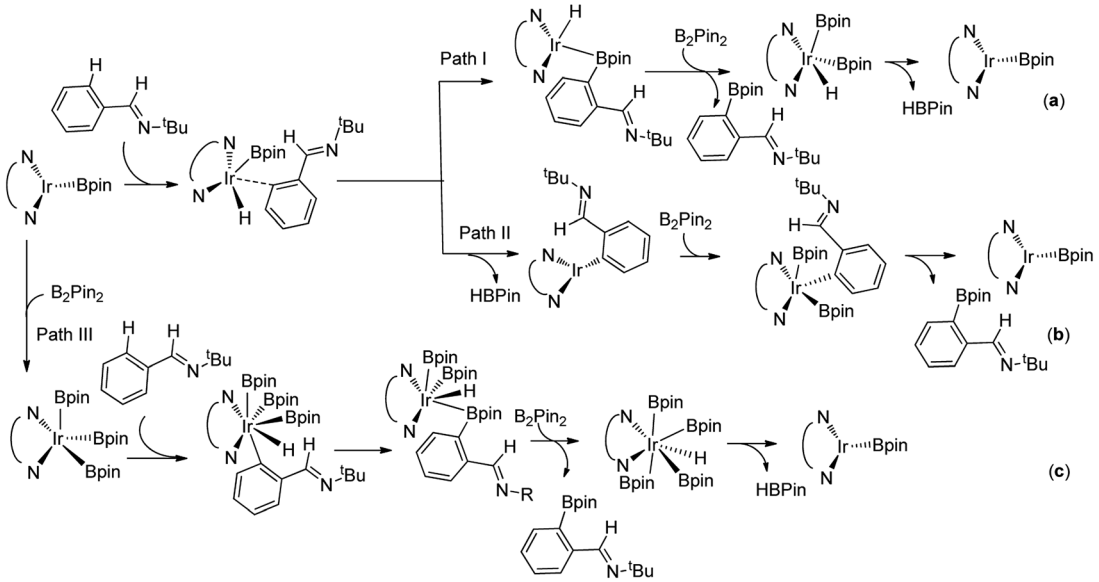

Scheme 2 Three types of potential mechanisms for C–H borylation of aromatic imine.

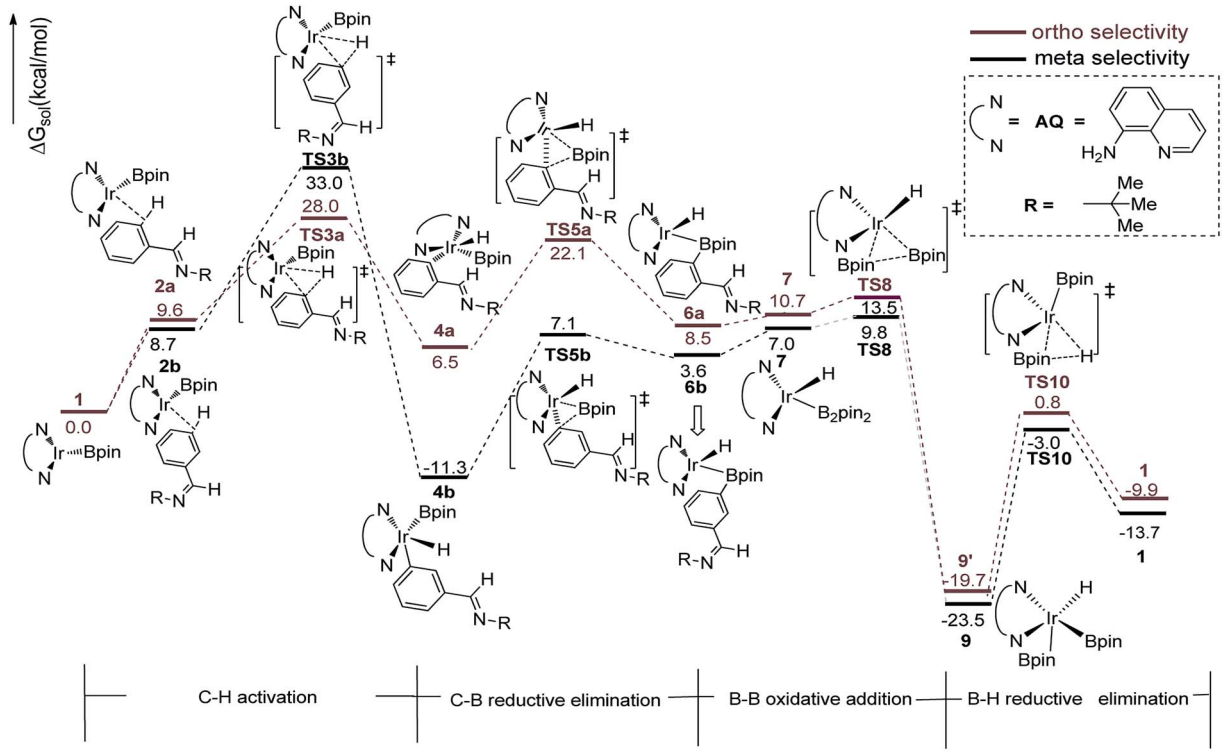

Fig. 2 Energy profile of path I in the borylation of aromatic imine catalyzed by AQ/Ir system.

Computational method

The followed DFT calculations have been conducted using Gaussian 09 program.[21] Geometries were optimized using the B3LYP functional.[22] SDD[23] basis set was used for Ir, a standard 6-31G(d)[24] basis set was used for other atoms. Frequency analyses were carried out to ensure theses stationary points were at either a minimum or transition state. Solvation free energies were calculated with SMD[25] solvation model (solvent = tetrahydrofuran). Additional single point calculations were performed with M11L functional.[26] SDD basis set was employed for Ir while standard 6-311++G(d,p)[24] basis set level for other atoms. The solvation model for the single point calculation was the same as described above. The energies presented in this paper are the M11L calculated single point energies added with B3LYP optimized thermodynamic corrections.

Results and discussion

We have first examined the borylation of aromatic imine with B_2pin_2 catalyzed by the Ir/AQ system (Scheme 1). The catalytic cycle starts with the step of C–H activation of substrate aromatic imine. The C–H bond is splitted upon the addition of H and C to the Ir center, affording intermediate **4a** or **4b** (Fig. 2). The corresponding barrier of C–H activation is 33.0 kcal mol^{-1} and 28.0 kcal mol^{-1} for the *meta*-C–H activation (**TS3b**, Fig. 2, black) and *ortho*-C–H activation (**TS3a**, Fig. 2, aubergine), respectively. Thereafter, we try to figure out which is more likely the second step in the catalytic cycle, the C–B reductive elimination or B–H reductive elimination?

We have calculated the possibility of C–B reductive elimination followed with the initial step of C–H activation. Upon C–H activation, B–C reductively eliminate from the intermediate **4a** or **4b** *via* **TS5a** or **TS5b** (Fig. 2), the barrier is 18.4 kcal mol^{-1} and 15.6 kcal mol^{-1} for *meta*- and *ortho*-selectivity, respectively (Fig. 2).

Then B–B oxidative addition to Ir center takes place to generate the iridium(III) complex. Two Ir–B distances of **TS8** (Fig. 2) are different (2.40 *vs.* 2.55 Å). The barrier for **TS8** is as low as 2.8 kcal mol^{-1}. The catalytic cycle is closed by B–H reductive elimination to regenerate catalyst **1** (**TS10**, Fig. 2), which requires 20.5 kcal mol^{-1}. Given that the barrier of transition states in initial C–H activation step is the highest along the route, C–H activation is likely the RDS step (regioselectivity determining step) in path I. Comparing *meta*-selectivity with

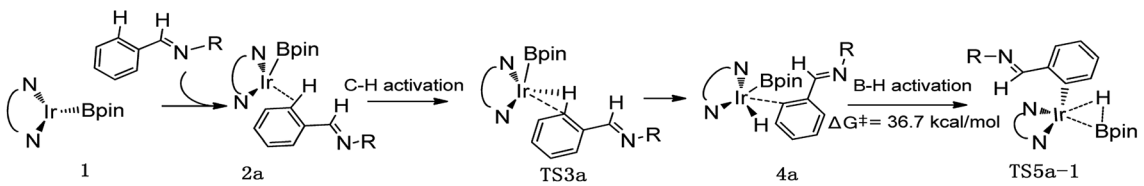

Scheme 3 Energy change in the second step of B–H reductive elimination for path II in AQ/Ir(I)-assisted C–H borylation of aromatic imine.

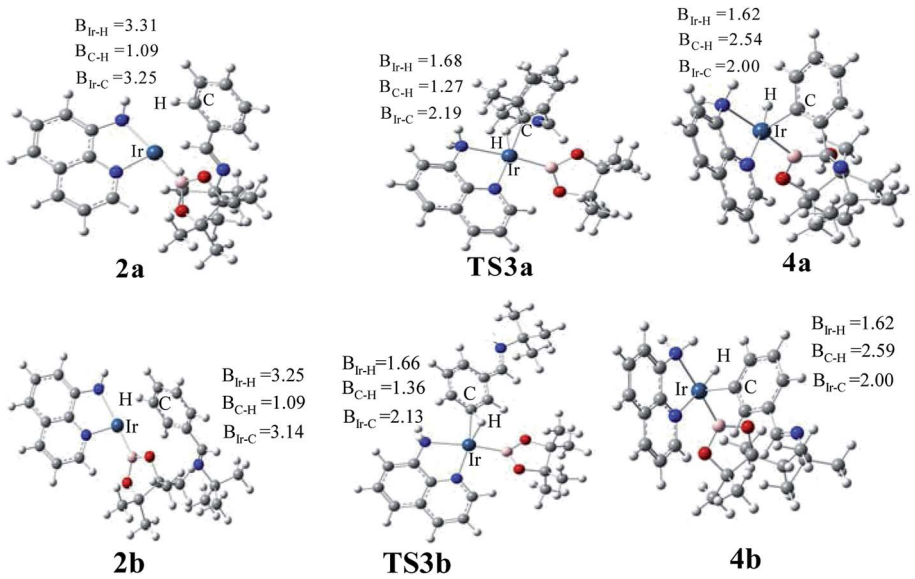

Fig. 3 Key transition states and intermediates in Ir(I)/AQ catalyzed C–H activation in path I.

ortho-selectivity in path I, our calculations indicate that *ortho* selectivity is favored over *meta* selectivity by 5.0 kcal mol^{-1} (33.0 kcal mol^{-1} *vs.* 28.0 kcal mol^{-1}) in the RDS step which is in consistent with experimental observation.[20]

Thereafter, we investigated an alternative of the second step, the B–H reductive elimination followed with C–H activation step (Scheme 2, path II). The barrier of B–H reductive elimination is 36.7 kcal mol^{-1} (Scheme 3). Because the barrier is too high to overcome under the experimental condition,[20] this pathway is ruled out, and further calculation along path II is abandoned.

The transition states of C–H activation and the related intermediates in path I are located and detailed in Fig. 3. For C–H activation, C–H of the phenyl ring approaches trans to boron and the C–H bond is splitted upon interaction between H, C and Ir atoms, resembling the previous studies by Sakaki.[27] According to the previous reports, boryl nucleophilicity promotes proton transfer in the transition state, thereby accelerates the subsequent C–H borylation.[28] During the process of C–H activation, both the length of Ir–C and Ir–H bond become shorter, and the length of C–H bond becomes longer. Comparing the transition states of TS3a and **TS3b**, which are

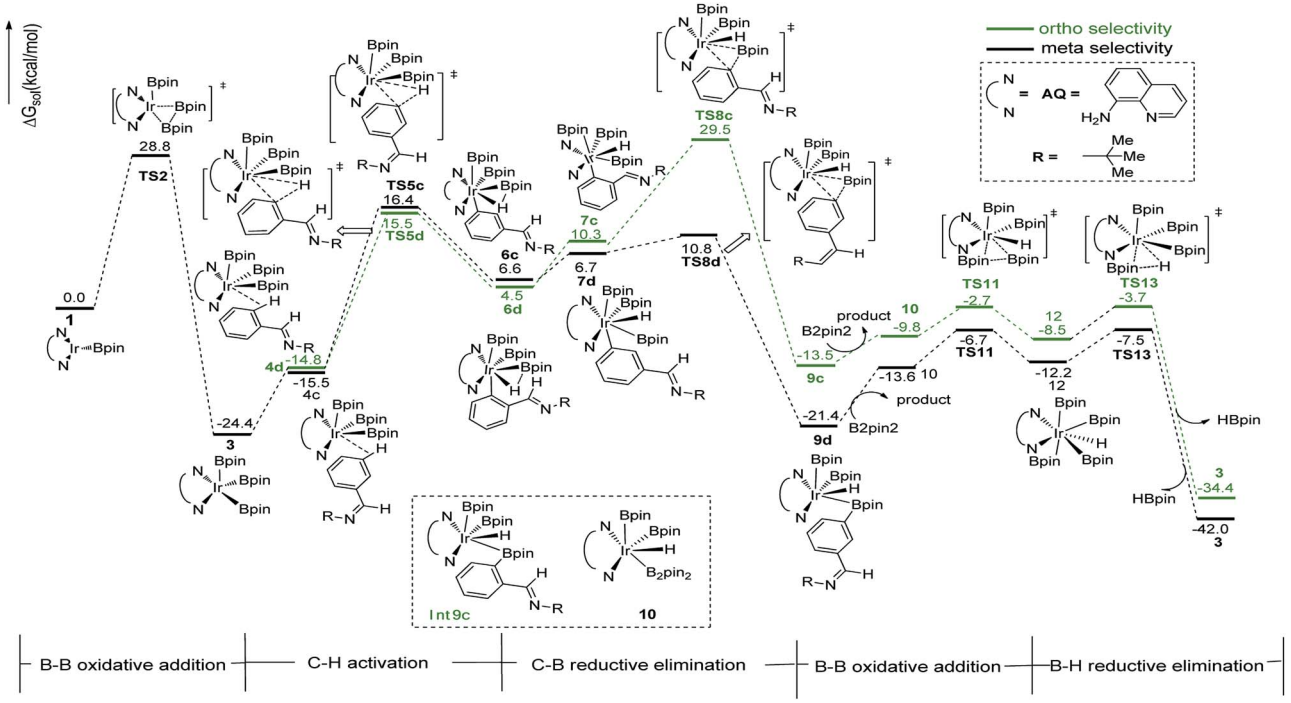

Fig. 4 Energy profile of path III in the borylation of aromatic imine catalyzed by TMP/Ir(I) system.

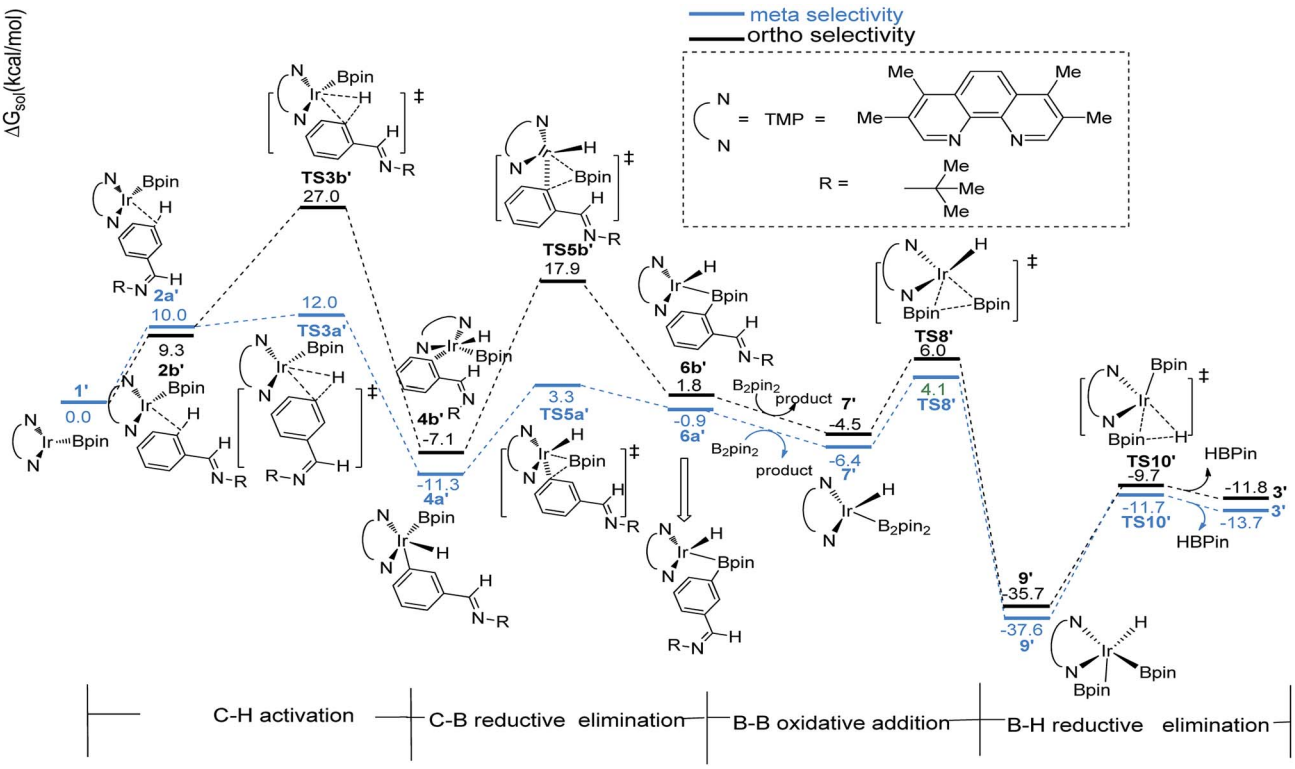

Fig. 5 Energy profile of path I′ in the borylation of aromatic imine catalyzed by TMP/Ir(I) system.

ortho- and *meta*-selectivity respectively, the latter is less steric hindrance. Surprisingly, the barrier of the larger hindered **TS3a** is lower. The lower energy of **TS3a** may due to the enhanced electron donating ability of AQ which accelerates the proton-transfer from *ortho* carbon to iridium atom.

The Ir(I)–Ir(III) catalytic cycle in path I bring us to envisage whether an analogous Ir(III)–Ir(V) pathway exists (Scheme 1c). The iridium center of precatalyst **1** is possible subjected to B–B oxidative addition with B_2pin_2 (Fig. 4). The barrier of the initial B–B oxidative addition step is slightly higher than that of *ortho* C–H activation in Ir(I)/Ir(III) cycle (**TS2** in Fig. 4 *vs.* **TS3a** in Fig. 2, 28.8 kcal mol^{-1} *vs.* 28.0 kcal mol^{-1}). Consequently, the B–B oxidative addition to iridium(I) should be a little more difficult to proceed than *ortho* C–H activation, therefore the B–B oxidative addition may not occur. Furthermore, we have calculated along the whole Ir(III)/Ir(V) route to testify the possibility of path III. The energy required for the initial aromatic C–H activation is higher than 35.0 kcal mol^{-1} for both *meta*- and *ortho*-selectivity (Fig. 4), much higher than the barrier for the analogous C–H activation step in Ir(I)–Ir(III) cycle. Therefore, this route is ruled out. We reach the conclusion that with ligand AQ, path I with *ortho*-selectivity is favoured over *meta*-selectivity, in consistent with the experimental observation.[20]

The similar pathways have been computed for the Ir(I)/TMP system. The energy profiles for the *ortho*-, and *meta*-borylation of aryl imine are shown in Fig. 5. In path I′, the total energy required for C–H activation is 12.0 kcal mol^{-1} and 27.0 kcal mol^{-1} for *meta*- and *ortho* borylation respectively (**TS3a**′ *vs.* **TS3b**′, Fig. 5). The followed C–B reductive elimination proceeds with a low barrier of 14.6 kcal mol^{-1} and 25.0 kcal mol^{-1} for *meta*- and *ortho*-selectivity. The subsequent B–B oxidative and B–H reductive elimination requires energy of 10.5 kcal mol^{-1} and 25.9 kcal mol^{-1} respectively, and finally regenerate catalyst **1**′. Given that the C–H oxidative addition step is the regioselectivity determining step, the lower energy barrier of *meta*-C–H activation than *ortho*-C–H activation indicates that *meta*-path I′ is preferred (27.0 kcal mol^{-1} *vs.* 12.0 kcal mol^{-1}).

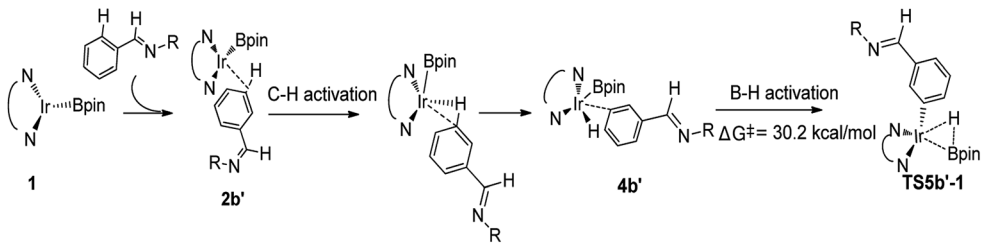

Scheme 4 Energy change in the second step of B–H reductive elimination for path II′ in TMP/Ir(I) assisted C–H borylation of aromatic imine.

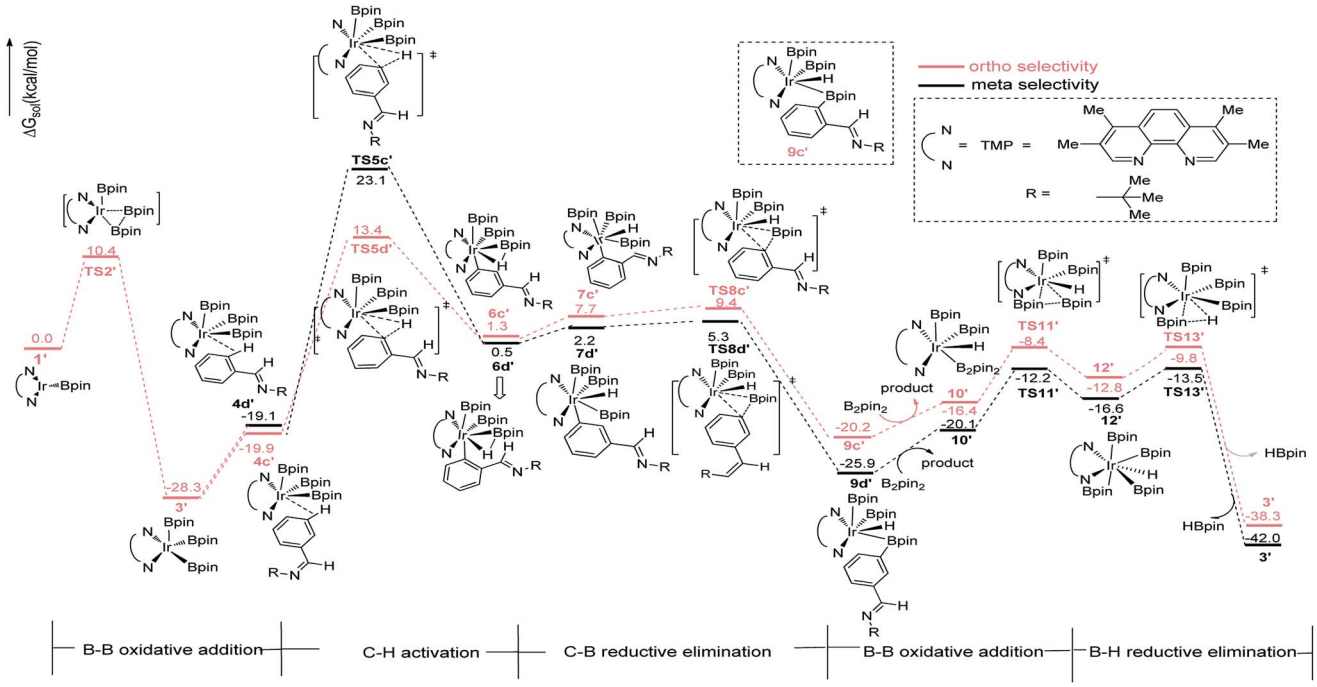

Fig. 6 Energy profile of path III′ in the borylation of aromatic imine catalyzed by TMP/Ir(III) system.

We then check another possibility that B–H reductive elimination is followed with the initial *meta*-C–H activation (Scheme 1, path II). As shown in Scheme 4, for *meta*-path II, the barrier of B–H reductive elimination is up to 30.2 kcal mol^{-1}, which is not possible to occur under experimental condition.[20] Therefore, path II′ is ruled out, and we have not continued to calculate this route.

In path III′, after B–B oxidative addition to Ir(I) which is the same as the first step in path III, the catalytic cycle proceeds with C–H activation, which requires energy of 42.2 kcal mol^{-1} and 33.3 kcal mol^{-1} for *meta*- and *ortho*-C–H activation. Thereafter, B–C bond reductively eliminates from intermediate **7a**′ or **7b**′ to produce **9a**′ or **9b**′ (Fig. 6). The required energy for this process is 3.1 kcal mol^{-1} and 1.7 kcal mol^{-1} for *meta*- and *ortho*-selectivity respectively. Then, B_2pin_2 adds to iridium center and the overall barrier for B–B oxidative addition is 8.0 kcal mol^{-1}. B–H reductive elimination *via* **13TS**′ leads to the regeneration of catalyst **1**′, with a low barrier of 3.0 kcal mol^{-1}. Overall, both *ortho*- and *meta*-path III′ have barriers higher than 30 kcal mol^{-1} for both *ortho*- and *meta*-selectivity, and it is not possible to occur under experimental conditions.[20] Therefore, path III′ is also ruled out.

The structure of transition states of C–H activation and related intermediates in path I′ are shown in Fig. 7. Structure

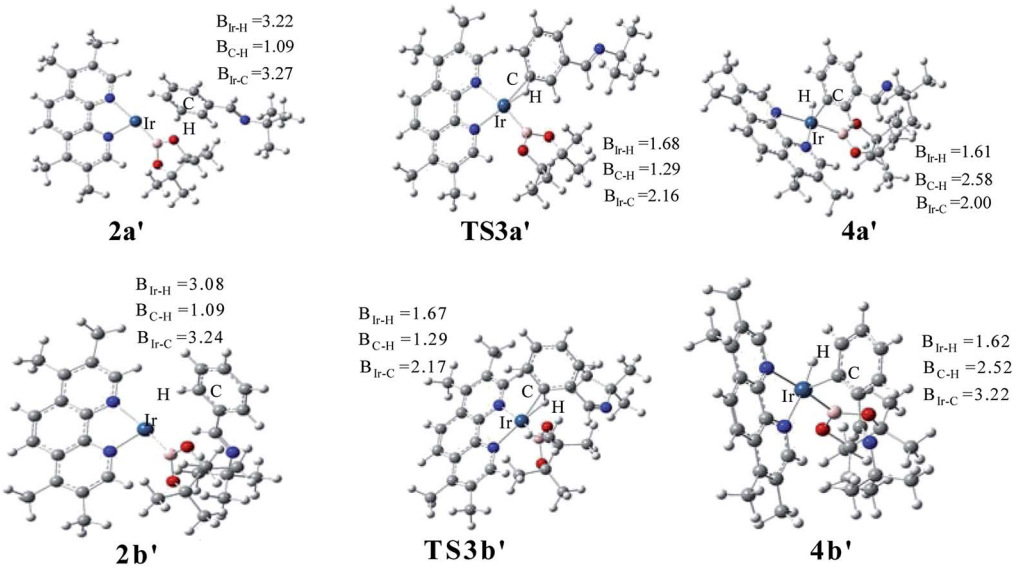

Fig. 7 Key transition states and intermediates in Ir(I)/TMP system catalyzed C–H activation in path I′.

comparison between **TS3a′** and **TS3b′** indicates that the lengths of the Ir–H, C–H, and Ir–C bonds in these two transition states are very similar to each other. The main difference lies in the steric repulsion between the boryl group and the substituted imine group. For **TS3b′**, the imine group are bent to retain stable structure, while for **TS3a′**, the imine substitutent on the aryl ring is unfolding, implying less steric hindrance than **TS3b′**. Therefore, the greater steric repulsion in transition states of orth C–H activation (**TS3b′**, Fig. 7) leads to higher energy barrier, making orth C–H activation more difficult than *meta* borylation.

The ligand-controlled selectivity can be rationalized by the combination of steric and electronic effects. The key factors that determine RDS step (C–H activation) are those accelerating transfer of hydrogen to Ir center. For TMP ligand, the *meta* product is obtained due to steric disfavor at *ortho* position. For AQ ligand, the decreased steric hindrance and strong electron donating ability of AQ promote *ortho* hydrogen transferring to iridium atom, while the electronic effects could be verified by different mulliken charge on atoms of **TS3a** and **TS3b′** (Table 1, ESI†). Accordingly, the *ortho*-selectivity attributes to the decreased steric hindrance and increased electron donating ability of AQ ligand while the *meta*-selectivity is due to the steric of TMP. This is in good consistent with the experimental observation.[20]

Conclusions

In summary, we have conducted DFT calculations to investigate the origins of the ligand controlled regioselectivity in iridium-catalyzed borylation of aromatic imine. The calculations are in satisfactory agreement with the experimentally observation. The results reveal a Ir(I)–Ir(III) catalytic cycle including four steps: (1) C–H oxidative addition, (2) B–C reductive elimination, (3) B–B oxidative addition and (4) B–H reductive elimination. The C–H oxidative addition is the regioselectivity determining step of the reaction. The structures of transition states in C–H activation step are analyzed to illustrate the different regioselectivity. For AQ ligand, the *ortho* product is shown to be favored over the *meta* product because of the decreased steric hindrance and increased electron donating effect of AQ ligand which promote proton transfer in *ortho* C–H activation. For TMP ligand, the unfavorable steric repulsion between TMP and the *ortho* substituted imine group results in a higher energy barrier for *ortho* transition state of C–H activation, therefore *meta* borylation is preferred.

The new mechanistic insights into the iridium catalyzed borylation of aromatic imines might be helpful to the understanding of the origin of ligand controlled regioselectivity in this kind of reaction, also provide guide for the design of new catalyst.

Conflicts of interest

There are no conflicts to declare.

Acknowledgements

We thank Natural Science Foundation of Guangdong Province (2017A030313020 and 2018A030313274) for financial support on this study. We also thank National Natural Science Foundation of China (11604059), the Priority Academic Program Development of Jiangsu Higher Education Institutions, China, Scientific Research Project of Guangzhou Municipal Colleges and Universities (1201630455) and the Guangzhou University's Training Program for Excellent New-recruited Doctors (YB201715).

Notes and references

1 (*a*) A. Ros, R. Fernandez and J. M. Lassaletta, *Chem. Soc. Rev.*, 2014, **43**, 3229; (*b*) J. F. Hartwig, *J. Am. Chem. Soc.*, 2016, **138**, 2; (*c*) L. Xu, G. Wang, S. Zhang, H. Wang, L. Wang, L. Liu, J. Jiao and P. Li, *Tetrahedron*, 2017, **73**, 7123; (*d*) I. Mkhalid, J. H. Barnard, T. B. Marder, J. M. Murphy and J. F. Hartwig, *Chem. Rev.*, 2010, **110**, 890; (*e*) D. G. Hall, Wiley-VCH: Weinheim, Germany, 2005; (*f*) G. R. Dick, E. M. Woerly and M. D. Burke, *Angew. Chem., Int. Ed.*, 2012, **51**, 2667.
2 C. Cheng and J. F. Hartwig, *Science*, 2014, **343**, 853.
3 J. V. Obligacion, S. P. Semproni and P. J. Chirik, *J. Am. Chem. Soc.*, 2014, **136**, 4133.
4 C. Xue, Y. Luo, H. L. Teng, Y. H. Ma, M. Nishiura and Z. M. Hou, *ACS Catal.*, 2018, **8**, 5017.
5 G. Wang, L. Liu, H. Wang, Y. Ding, J. Zhou, S. Mao and P. Li, *J. Am. Chem. Soc.*, 2017, **139**, 91.
6 B. Chattopadhyay, J. E. Dannatt, I. L. A. D. Sanctis, K. A. Gore, R. E. Maleczka, D. A. Singleton and M. R Smith, *J. Am. Chem. Soc.*, 2017, **139**, 7864.
7 (*a*) H. L. Li, M. Kanai and Y. Kuninobu, *Org. Lett.*, 2017, **19**, 5944; (*b*) M. R. Smith, R. Bisht, C. Haldar, G. Pandey, J. E. Dannatt, B. Ghaffari, R. E. Maleczka and B. Chattopadhyay, *ACS Catal.*, 2018, **8**, 6216; (*c*) C. Haldar, M. E. Hoque, R. Bisht and B. Chattopadhyay, *Tetrahedron Lett.*, 2018, **59**, 1269; (*d*) M. T. Mihai, H. J. Davis, G. R. Genov and R. J. Phipps, *ACS Catal.*, 2018, **8**, 3764.
8 (*a*) A. Ros, B. Estepa, R. Lopez-Rodroguez, E. Alvarez, R. Fernandez and J. M. Lassaletta, *Angew. Chem., Int. Ed.*, 2011, **50**, 11724; (*b*) P. C. Roosen, V. A. Kallepalli, B. Chattopadhyay, D. A. Singleton, R. E. Maleczka and M. R. Smith, *J. Am. Chem. Soc.*, 2012, **134**, 11350; (*c*) R. Bisht and B. Chattopadhyay, *J. Am. Chem. Soc.*, 2016, **138**, 84.
9 (*a*) S. Kawamorita, H. Ohmiya, K. Hara, A. Fukuoka and M. Sawamura, *J. Am. Chem. Soc.*, 2009, **131**, 5058; (*b*) T. Ishiyama, H. Isou, T. Kikuchi and N. Miyaura, *Chem. Commun.*, 2010, **46**, 159.
10 M. A. Larsen, S. H. Cho and J. Hartwig, *J. Am. Chem. Soc.*, 2016, **138**, 762.
11 G. A. Chotana, M. A. Rak and M. R. Smith, *J. Am. Chem. Soc.*, 2005, **127**, 10539.
12 R. E. Maleczka, F. Shi, D. Holmes and M. R. Smith, *J. Am. Chem. Soc.*, 2003, **125**, 7792.
13 J. M. Murphy, X. Liao and J. F. Hartwig, *J. Am. Chem. Soc.*, 2007, **129**, 15434.
14 H. Tamura, H. Yamazaki, H. Sato and S. Sakaki, *J. Am. Chem. Soc.*, 2003, **125**, 16114.

15 T. M. Boller, J. M. Murphy, M. Hapke, T. Ishiyama, N. Miyaura and J. F. Hartwig, *J. Am. Chem. Soc.*, 2005, **127**, 14263.
16 A. G. Green, P. Liu, C. A. Merlic and K. N. Houk, *J. Am. Chem. Soc.*, 2014, **136**, 4575.
17 J. Jover and F. Maseras, *Organometallics*, 2016, **35**, 3221.
18 L. Zhu, X. T. Qi, Y. Z. Li, M. Duan, L. F. Zou, R. P. Bai and Y. Lan, *Organometallics*, 2017, **36**, 2107.
19 T. M. Boller, J. M. Murphy, M. Hapke, T. Ishiyama, N. Miyaura and J. F. Hartwig, *J. Am. Chem. Soc.*, 2005, **127**, 14263.
20 R. Bisht and B. Chattopadhyay, *J. Am. Chem. Soc.*, 2016, **138**, 84.
21 M. J. Frisch, G. W. Trucks, H. B. Schlegel, G. E. Scuseria, M. A. Robb, J. R. Cheeseman, G. Scalmani, V. Barone, B. Mennucci, G. A. Petersson, H. Nakatsuji, M. Caricato, X. Li, H. P. Hratchian, A. F. Izmaylov, J. Bloino, G. Zheng,J. L. Sonnenberg, M. Hada, M. Ehara, K. Toyota, R. Fukuda, J. Hasegawa, M. Ishida, T. Nakajima, Y. Honda, O. Kitao, H. N. akai, T. Vreven, J. A. Montgomery Jr, J. E. Peralta, F. Ogliaro, M. Bearpark, J. J. Heyd, E. Brothers, K. N. Kudin, V. N. Staroverov, R. Kobayashi, J. Normand, K. Raghavachari, A. Rendell, J. C. Burant, S. S. Iyengar, J. Tomasi, M. Cossi, N. Rega, J. M. Millam, M. Klene, J. E. Knox, J. B. Cross, V. Bakken, C. Adamo, J. Jaramillo, R. Gomperts, R. E. Stratmann, O. Yazyev, A. J. Austin, R. Cammi, C. Pomelli, J. W. Ochterski, R. L. Martin, K. Morokuma, V. G. Zakrzewski, G. A. Voth, P. Salvador, J. J. Dannenberg, S. Dapprich, A. D. Daniels, Ö. Farkas, J. B. Foresman, J. V. Ortiz, J. Cioslowski, D. J. Fox, *Gaussian 09*, Gaussian, Inc., Wallingford CT, 2009.
22 (*a*) C. Lee, W. Yang and R. G. Parr, *Phys. Rev. B: Condens. Matter Mater. Phys.*, 1988, **37**, 785; (*b*) A. D. Becke, *J. Chem. Phys.*, 1993, **98**, 5648.
23 M. Dolg, U. Wedig, H. Stoll and H. Preuss, *J. Chem. Phys.*, 1987, **86**, 866.
24 (*a*) P. C. Hariharan and J. A. Pople, *Theor. Chem. Acc.*, 1973, **28**, 213; (*b*) M. J. Frisch, J. A. Pople and J. S. Binkley, *J. Chem. Phys.*, 1984, **80**, 3265.
25 A. V. Marenich, C. J. Cramer and D. G. Truhlar, *J. Phys. Chem. B*, 2009, **113**, 6378.
26 R. Peverati and D. G. Truhlar, *J. Phys. Chem. Lett.*, 2012, **3**, 117.
27 H. Tamura, H. Yamazaki, H. Sato and S. Sakaki, *J. Am. Chem. Soc.*, 2003, **125**, 16114.
28 B. A. Vanchura, S. M. Preshlock, P. C. Roosen, V. A. Kallepalli, R. J. Staples, R. E. Maleczka and M. R. Smith, *Chem. Commun.*, 2010, **46**, 7724.